Mesoporous Materials

DOI: 10.1002/anie.201002849

# A Low-Concentration Hydrothermal Synthesis of Biocompatible Ordered Mesoporous Carbon Nanospheres with Tunable and Uniform Size**

*Yin Fang, Dong Gu, Ying Zou, Zhangxiong Wu, Fuyou Li, Renchao Che, Yonghui Deng, Bo Tu, and Dongyuan Zhao**

Nanoparticles with ordered mesostructures benefit from advantages resulting from the remarkable and complementary property of the mesochannels and quantum effects in the nanoscale. Their open-framework structures, large surface area and porosity, and nanosize make ordered mesoporous nanoparticles useful in adsorption,[1–3] controlled drugs release,[4–9] cellular delivery,[10–16] energy storage,[17–22] and catalysis.[23] Among mesoporous nanoparticles, silicates have been extensively synthesized by a well-controllable process based on sol–gel chemistry. Mesoporous carbon materials have many advantages over silica materials, such as electrical conductivity, chemical inertness, hydrophobic property, which enable them to be widely used as supercapacitors,[17,18] fuel cells,[19,20] lithium batteries,[22] and hydrophobic drugs carriers.[12] Similar to silica, carbon nanoparticles are nontoxic, biocompatible, and nonimmunogenic, which allows them to be used extensively in cellular delivery.[15,16] Therefore, many efforts have been made to fabricate mesoporous carbon nanoparticles. In general, a nanocasting strategy was adopted by employing nanosized mesoporous silica as a hard template.[15,24–29] Nevertheless, nanocasting is a very fussy, high-cost, and thus industrial unfeasible method.[30] Also, the mesostructures and morphologies of the replicated carbon nanoparticles are limited to the parent silica template. However, small mesoporous carbon nanoparticles are difficult to obtain by hard-templating approach because of the aggregation and cross-linking tendency of the nanosized silicate templates and the carbon resource.[10,11] Recently, an organic–organic assembly method has been successfully developed to synthesize ordered mesoporous carbons with various structures by using amphiphilic triblock copolymers as a soft template and phenolic resol as a carbon source.[31–37] Two routes can be used to prepare the mesoporous carbon materials, one is the well-known evaporation induced self-assembly (EISA) method in ethanol solution, and another is aqueous solution route under a "hydrothermal"[38–41] conditions at a low temperature of 60–70 °C. Morphologies of the mesoporous carbon materials synthesized from the EISA strategy are usually films and monolithic, whereas the aqueous route usually yields powder carbon materials with particle sizes in the micrometer or millimeter scale. More recently, mesoporous carbon microspheres with the diameter over 50 μm were synthesized by a suspension assisted method, which was developed by Long and co-workers.[42] In this work, the spherical diameters were limited to micrometer-sized emulsion droplets. In this case, ordered mesoporous carbon nanoparticles are difficult to synthesize under the present conditions. To the best of our knowledge, there are no reports of the direct synthesis of ordered mesoporous carbon nanoparticles, especially nanospheres with uniform size.

Herein, we demonstrate a novel low-concentration hydrothermal route to synthesize highly ordered body-centered cubic ($Im\bar{3}m$) mesoporous carbon nanoparticles with spherical morphology and uniform size. Commercial available triblock copolymer Pluronic F127 was employed as a template and phenolic resol as a carbon source. A low-concentration (ca. $10^{-7}$ mol $L^{-1}$ surfactant) controlled hydrothermal treatment was carried out to obtain the nanostructure and confine the particle size. The ordered mesostructures were retained while the spherical diameters were tuned from 20 to 140 nm by simply varying the reagent concentration. Small-sized nanospheres with diameters of around 20 nm, of which the boundary approaches only one mesostructural unit cell, were observed for first time. This method may reveal a possible alternative to "classical" methods for the preparation of carbon nanostructures and in some cases, the only viable synthetic route toward certain carbon nanostructures. The obtained mesoporous carbon nanospheres show no high cytotoxicity, good cellar permeability, and high drug capacity, which is greatly potential in prospected application of cellar delivery and cell imaging.

Scanning electron microscopy (SEM) images (Figure S1 in the Supporting Information) show that the four representative samples synthesized by the low-concentration hydrothermal approach, which are assigned as MCN-140, MCN-90, MCN-50, and MCN-20 (MCN denotes Mesoporous Carbon

[*] Y. Fang, D. Gu, Y. Zou, Z. X. Wu, Prof. Dr. F. Y. Li, Prof. Dr. R. C. Che, Prof. Dr. Y. H. Deng, Prof. Dr. B. Tu, Prof. Dr. D. Y. Zhao
Laboratory of Advanced Materials, Department of Chemistry and Shanghai Key Laboratory of Molecular Catalysis and Innovative Materials
Fudan University, Shanghai 200433 (P.R. China)
Fax: (+86) 21-5163-0307
E-mail: dyzhao@fudan.edu.cn
Homepage: http://homepage.fudan.edu.cn/~dyzhao/default.htm

[**] This work was supported by the NSF of China (20721063, 20821140537, and 20871030), the State Key Basic Research Program of the People's Republic of China (2006CB932302, 2009AA033701, and 2009CB930400), the Shanghai Leading Academic Discipline Project (B108), the Shanghai Nanotech Promotion Center (0852nm00100), the Science and Technology Commission of Shanghai Municipality (08DZ2270500), and the Fudan Graduate Innovation Funds.

Supporting information for this article is available on the WWW under http://dx.doi.org/10.1002/anie.201002849.

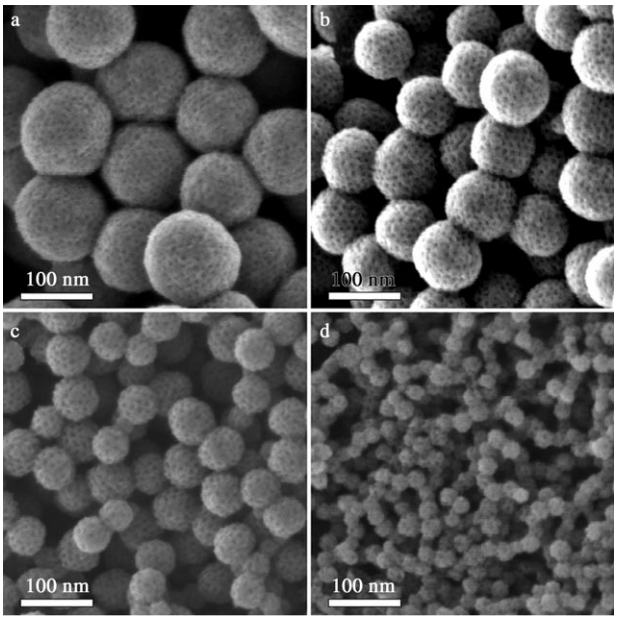


***Figure 1.*** HRSEM images of the ordered mesoporous carbon nanospheres prepared by a low-concentration hydrothermal method at 130 °C: a) MCN-140 with a diameter of 140 nm; b) MCN-90 with a diameter of 90 nm; c) MCN-50 with a diameter of 50 nm, and d) MCN-20 with a diameter of 20 nm.

Nanospheres, the number gives the particle size in nanometers), have uniform spherical morphology in large domains. A high-resolution SEM (HRSEM) image (Figure 1a) shows that the sample MCN-140 synthesized at a high phenol/water ratio of 1:200 contains uniform spheres with a size of approximately 140 nm. The carbon nanospheres are separated from each other. It is remarkable that an ordered hexagonal array of mesopores can be clearly observed from the exposed hemispheres, implying an open pore structure on the surface. The pore size is roughly estimated to be about 3 nm. The number of mesopores exposed on the hemispherical surface can be roughly counted to be around 160. The diameter of the mesoporous carbon spheres decreases from 140 to 20 nm as the molar ratio of phenol/water decreases from 1:200 to 1:450 (Figure 1). Mesopores exposed on the surface of the carbon spheres of MCN-90, MCN-50, and MCN-20 can be roughly counted and were found to be 70, 40, and 4, respectively. It is noticeable that only 4 mesopores can be observed for the sample MCN-20 (Figure 1d), suggesting the smallest diameter of the ordered mesoporous nanosphere, which approaches to one unit cell of body-centered cubic mesostructure.

The small-angle X-ray scattering (SAXS) pattern of the mesoporous carbon nanospheres MCN-140 shows two resolved scattering peaks at $q$ values of 0.73 and 1.27 $nm^{-1}$ (Figure S2a in the Supporting Information). The peaks with the $q$ ratio of $1:\sqrt{3}$ can be indexed as the 110 and 211 reflections of a body-centered cubic $Im\bar{3}m$ mesostructure. As the particle sizes decrease, the scattering peaks degrade and become broad (Figure S2b–d), probably as a result of the decrease of the ordered mesopore domain size.

A transmission electron microscopy (TEM) image (Figure 2a) of mesoporous carbon MCN-140 shows uniform isolated spheres with diameters of approximately 140 nm, which corresponds well with the HRSEM results. TEM images viewed along [111] and [110] directions (Figure 2a insert) further confirm a body-centered cubic mesostructure with space-group $Im\bar{3}m$ symmetry. The pore size can be roughly measured to be 2.6 nm, which is close to that from the HRSEM results.

With the decrease in particle size, the ordered mesopore arrangement can also be observed from the TEM images (Figure 2b–d). The carbon nanospheres tend to congregate together when the particle size decreases to 20 nm. Furthermore, only 3–5 mesopores can be seen from the high-resolution TEM (HRTEM) image (Figure 2d insert), further suggesting one unit cell of $Im\bar{3}m$ mesostructure in one particle.

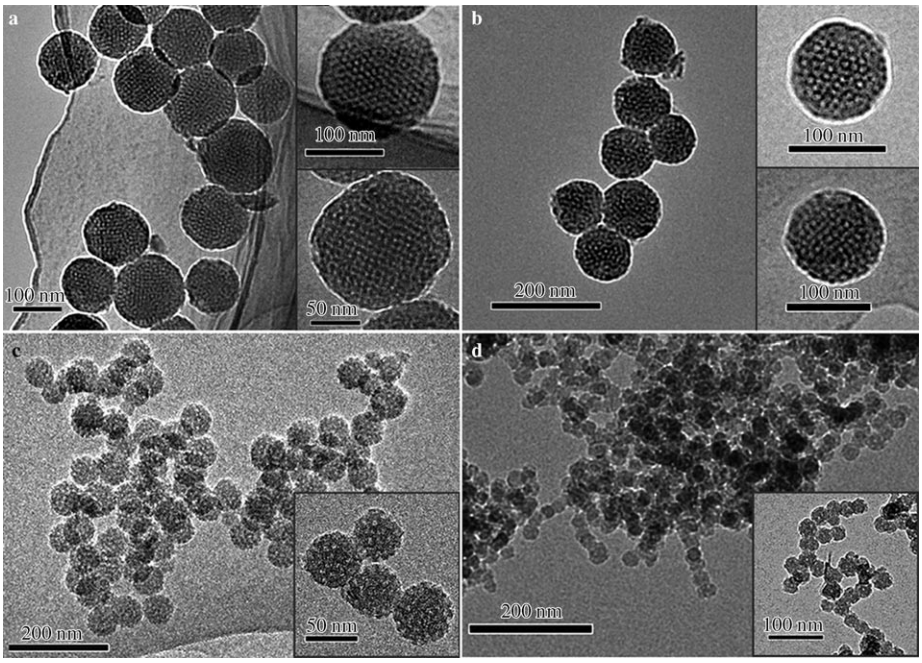


***Figure 2.*** TEM images of the mesoporous carbon nanospheres with different particle sizes: a) 140 nm (MCN-140); HRTEM images viewed along [111] (top insert) and [110] (bottom insert) directions; b) 90 nm (MCN-90); HRTEM images viewed along [111] (top insert) and [110] (bottom insert) directions; c) 50 nm (MCN-50); HRTEM image (insert); d) 20 nm (MCN-20); HRTEM image (insert). The molar ratios of phenol/water in the synthesis batches for the samples MCN-140, MCN-90, MCN-50, and MCN-20 are 1:200, 1:250, 1:320, and 1:450, respectively.

  

$N_2$ sorption isotherms of the mesoporous carbon nanosphere MCN-140 shows pseudo-type-I curve with H1 hysteresis loop at high relative pressure (Figure S3A in the Supporting Information). This behavior is typically associated with micropores and mesopores. An indistinct capillary condensation step at $P/P_0 = 0.20$–$0.40$ was observed, which is typical of small mesopores. Moreover, a hysteresis loop at a higher pressure ($P/P_0 = 0.9$–$0.993$) may reflect the interparticle texture between the carbon nanospheres. The pore size distributions were calculated by a density functional theory (DFT) model from the adsorption branches of the isotherms to be approximately 2.6 nm for the sample MCN-140, which agrees well with that evaluated from TEM images. Similar to the sample MCN-140, the $N_2$ sorption isotherms of the samples MCN-90, MCN-50, and MCN-20 follow similar behavior, showing pseudo-type-I curves with H1 hysteresis loop at the high relative pressure. The pore sizes were calculated to be 2.6–3.0 nm (Figure S3B). The BET surface areas of these carbon spheres are in the range 894–1131 $m^2 g^{-1}$ (Table 1), which are a little higher than that of the mesoporous carbon material FDU-16 synthesized in aqueous solution at a low temperature (66–70 °C).[35] The pore volumes were calculated to be as large as 1.0–1.5 $cm^3 g^{-1}$, which are also much larger than that of FDU-16 (0.3–0.6 $cm^3 g^{-1}$). The larger pore volume is probably a result of the easier removal of the templates from the spherical mesoporous carbons with small particle size and their more open accessible mesopores. However, the latter sample (FDU-16) with thick pore walls and remarkable pore shrinkage shows much lower pore volume.

On the basis of the above observations, we propose a low-concentration growth and hydrothermal reaction promoted assembly process to explain the formation of ordered mesoporous carbon nanospheres (Figure 3). Spherical phenolic resol-F127 monomicelles are formed first from the hydrogen-bond interaction between pluronic F127 and resols under low-concentration conditions. The reactant is controlled at low concentration ($10^{-7}$ mol $L^{-1}$) to avoid the excessive cross-linking between micelles. During the high temperature (130 °C) hydrothermal process, the F127/resol spherical monomicelles can be promoted to further assemble the low-energy cubic closed packing mesostructure (space group $Im\bar{3}m$) with the further cross-linking of phenolic resols. Because the cross-linking process occurs actively at the high temperature and the crystal growth is isotropic, a spherical morphology is obtained. Simultaneously, the high-temperature hydrothermal treatment drives the small spherical micelles to accumulate and rearrange while polymerization of the resols is occurring inside the spheres. As a result, a large spherical F127/resol composite with ordered cubic mesostructure is formed, leaving behind the open and accessible mesopore array on the surface. The lower the concentration of reagents, the fewer monomicelles are assembled in the reachable domain, resulting in a smaller diameter of the mesoporous carbon spheres.

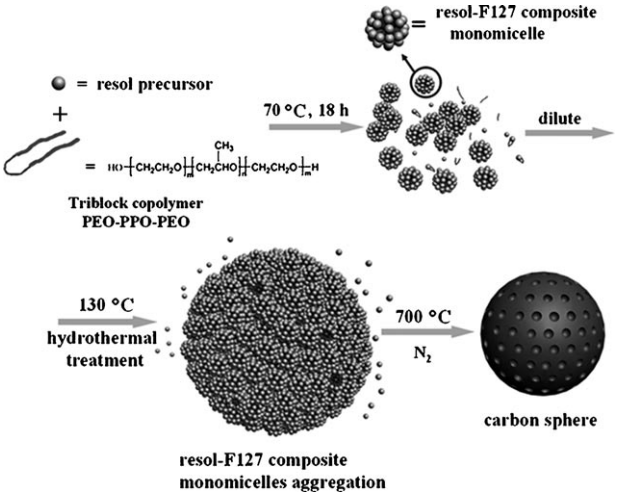


***Figure 3.*** Formation process of the uniform ordered mesoporous carbon nanospheres (particle size controlled by concentration).

The cell permeability of the obtained carbon nanoparticles was investigated by using fluorescein isothiocyanate (FITC) as a tracer. After incubation with a MEM (modified eagle medium) solution of the functional mesoporous carbon nanospheres (FITC-MCN-90) for 2 h at 25 °C (see the Supporting Information), a remarkable intracellular luminescence was observed in the confocal laser scanning microscopy (CLSM) image of KB (human nasopharyngeal epiclermal carcinoma) cells (Figure 4a). The overlaid images show that the luminescence is from the cytoplasm of the cells, implying that the mesoporous carbon nanospheres can enter into the living cells (Figure 4c). This result was further confirmed by differential interference contrast (DIC) microscopy (Figure S6 in the Supporting Information). The cell permeability measurements show that all of the samples MCN-90, MCN-50, and MCN-20 can penetrate into the living cells (Figure S7), suggesting a potential application in cellar delivery and cell imaging. Measurements of the cell viability by the methyl thiazolyl tetrazolium (MTT) assay (Figure 4d) reveals that after culturing in 1–100 μM of the mesoporous carbon nanoparticles for 6 h, the cell viability remains above 90%. Even after culturing for 24 h, less than 10% of the KB cells died in the presence of a relatively high concentration

***Table 1:*** Physicochemical properties of the ordered mesoporous carbon nanospheres with different particle sizes.

| Sample | Particle size [nm] | Cell parameter *a* [nm][a] | Pore size [nm][b] | Pore volume [$cm^3 g^{-1}$] | BET surface area [$m^2 g^{-1}$][c] | Micropore volume [$cm^3 g^{-1}$][d] |
|---|---|---|---|---|---|---|
| MCN-140 | 140±10 | 12.1 | 2.6 | 1.11 | 941 | 0.26 |
| MCN-90 | 90±10 | 12.2 | 2.6 | 1.52 | 1131 | 0.31 |
| MCN-50 | 50±5 | 12.7 | 2.6 | 1.38 | 993 | 0.27 |
| MCN-20 | 20±5 | 13.0 | 3.0 | 1.32 | 894 | 0.24 |

[a] Calculated from the SAXS results. [b] Calculated by the DFT model from the adsorption branches of the isotherms. [c] Calculated by the multipoint BET model from adsorption data. [d] Calculated by the *V*–*t* plot method.

  

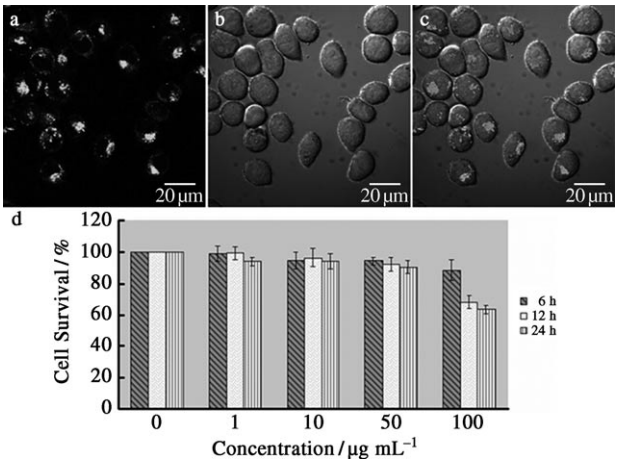


***Figure 4.*** a) Confocal laser scanning microscope image of KB living cells incubated with a MEM solution of the functional mesoporous carbon nanospheres FITC-MCN-90 (MCN-90 grafted with fluorescein isothiocyanate) for 2 h at 25 °C ($\lambda_{ex}$ = 488 nm); b) the corresponding bright-field image of the cells; c) an overlay image of (a) and (b); d) cell viability values (%) estimated by MTT assay in KB cells, which were cultured in the presence of 1–100 μM MCN-90 at 37 °C for 6–24 h.

($50\ \mu g\,mL^{-1}$) of the mesoporous carbon material. When the concentration increases to $100\ \mu g\,mL^{-1}$, the cell viability remained above 65%. These results suggest that the nanospheres seem not to be highly cytotoxic.

The drug adsorption capacity of the mesoporous carbon nanospheres was investigated by using ibuprofen as a probe (Figure S8 in the Supporting Information). The adsorption amount of ibuprofen in organic solvent was found to increase as the concentration of mesoporous carbon nanospheres increases, and the largest quantity reached $30\ mg\,g^{-1}$ in a short time, demonstrating a good adsorption capacity. This result also implies that the mesopores are open and accessible.

In summary, we demonstrated a novel low-concentration hydrothermal approach to ordered mesoporous carbon nanospheres with uniform diameter and body-centered cubic $Im\bar{3}m$ symmetry. The synthesis with high yield (61.6%) can be carried out on a relatively large scale (grams) by using pluronic F127 as a template and phenolic resol as a carbon source at around 70 °C. The obtained mesoporous carbon nanospheres have high surface area (ca. $1131\ m^2\,g^{-1}$) and large pore volume ($1.52\ cm^3\,g^{-1}$). A spherical monomicelle assembly process promoted by high-temperature hydrothermal treatment at 130 °C is proposed. The particle size of the carbon nanospheres is uniform and easily tunable from 20 to 140 nm by simply varying the reactant concentrations. The ordered mesopore arrays can be clearly observed by HRSEM images on the surface, suggesting that they are open and accessible. The smallest diameter (ca. 20 nm) of an ordered mesoporous sphere is demonstrated; there are only 9 mesopores (one mesostructual unit) in one sphere. The resultant mesoporous carbon nanospheres show low cytotoxicity and excellent cell permeability. The results reveal that this kind of material could be used in biological fields such as cell imaging and cellar drug delivery.

Received: May 11, 2010
Published online: September 13, 2010

**Keywords:** carbon · drug delivery · hydrothermal synthesis · mesoporous materials · nanoparticles

[1] Z. D. Lu, M. M. Ye, N. Li, W. W. Zhong, Y. D. Yin, *Angew. Chem.* **2010**, *122*, 1906; *Angew. Chem. Int. Ed.* **2010**, *49*, 1862.
[2] R. J. Tian, H. Zhang, M. L. Ye, X. G. Jiang, L. H. Hu, X. Li, X. H. Bao, H. F. Zou, *Angew. Chem.* **2007**, *119*, 980; *Angew. Chem. Int. Ed.* **2007**, *46*, 962.
[3] K. Ariga, A. Vinu, M. Miyahara, J. P. Hill, T. Mori, *J. Am. Chem. Soc.* **2007**, *129*, 11022.
[4] R. Liu, Y. Zhang, X. Zhao, A. Agarwal, L. J. Mueller, P. Y. Feng, *J. Am. Chem. Soc.* **2010**, *132*, 1500.
[5] J. E. Lee, N. Lee, H. Kim, J. Kim, S. H. Choi, J. H. Kim, T. Kim, I. C. Song, S. P. Park, W. K. Moon, T. Hyeon, *J. Am. Chem. Soc.* **2010**, *132*, 552.
[6] S. Gai, P. Yang, C. Li, W. Wang, Y. Dai, N. Niu, J. Lin, *Adv. Funct. Mater.* **2010**, *20*, 1166.
[7] Y. N. Zhao, B. G. Trewyn, I. I. Slowing, V. S. Y. Lin, *J. Am. Chem. Soc.* **2009**, *131*, 8398.
[8] I. I. Slowing, J. L. Vivero-Escoto, C. W. Wu, V. S. Y. Lin, *Adv. Drug Delivery Rev.* **2008**, *60*, 1278.
[9] C. Park, K. Oh, S. C. Lee, C. Kim, *Angew. Chem.* **2007**, *119*, 1477; *Angew. Chem. Int. Ed.* **2007**, *46*, 1455.
[10] Y. S. Lin, C. L. Haynes, *J. Am. Chem. Soc.* **2010**, *132*, 4834.
[11] F. Lu, S. H. Wu, Y. Hung, C. Y. Mou, *Small* **2009**, *5*, 1408.
[12] J. Lu, M. Liong, J. I. Zink, F. Tamanoi, *Small* **2007**, *3*, 1341.
[13] N. W. S. Kam, Z. A. Liu, H. J. Dai, *Angew. Chem.* **2006**, *118*, 591; *Angew. Chem. Int. Ed.* **2006**, *45*, 577.
[14] J. Kim, H. S. Kim, N. Lee, T. Kim, H. Kim, T. Yu, I. C. Song, W. K. Moon, T. Hyeon, *Angew. Chem.* **2008**, *120*, 8566; *Angew. Chem. Int. Ed.* **2008**, *47*, 8438.
[15] T. W. Kim, P. W. Chung, I. I. Slowing, M. Tsunoda, E. S. Yeung, V. S. Y. Lin, *Nano Lett.* **2008**, *8*, 3724.
[16] A. H. Yan, B. W. Lau, B. S. Weissman, I. Kulaots, N. Y. C. Yang, A. B. Kane, R. H. Hurt, *Adv. Mater.* **2006**, *18*, 2373.
[17] H. J. Liu, W. J. Cui, L. H. Jin, C. X. Wang, Y. Y. Xia, *J. Mater. Chem.* **2009**, *19*, 3661; Y. Wan, Y. F. Yang, D. Y. Zhao, *Chem. Mater.* **2008**, *20*, 932.
[18] W. R. Li, D. H. Chen, Z. Li, Y. F. Shi, Y. Wan, J. J. Huang, J. J. Yang, D. Y. Zhao, Z. Y. Jiang, *Electrochem. Commun.* **2007**, *9*, 569.
[19] H. Chang, S. H. Joo, C. Pak, *J. Mater. Chem.* **2007**, *17*, 3078.
[20] Z. Y. Yuan, B. L. Su, *J. Mater. Chem.* **2006**, *16*, 663.
[21] F. B. Su, J. H. Zeng, X. Y. Bao, Y. S. Yu, J. Y. Lee, X. S. Zhao, *Chem. Mater.* **2005**, *17*, 3960.
[22] Y. G. Guo, Y. S. Hu, J. Maier, *Chem. Commun.* **2006**, 2783.
[23] C. Li, *Catal. Rev.* **2004**, *46*, 419.
[24] X. Yan, H. H. Song, X. H. Chen, *J. Mater. Chem.* **2009**, *19*, 4491.
[25] Z. Y. Wang, F. Li, A. Stein, *Nano Lett.* **2007**, *7*, 3223.
[26] J. Ren, J. Ding, K. Y. Chan, H. T. Wang, *Chem. Mater.* **2007**, *19*, 2786.
[27] Y. D. Xia, Z. X. Yang, R. Mokaya, *Chem. Mater.* **2006**, *18*, 140.
[28] J. E. Hampsey, Q. Y. Hu, L. Rice, J. B. Pang, Z. W. Wu, Y. F. Lu, *Chem. Commun.* **2005**, 3606.
[29] A. B. Fuertes, *J. Mater. Chem.* **2003**, *13*, 3085.
[30] H. F. Yang, D. Y. Zhao, *J. Mater. Chem.* **2005**, *15*, 1217; Y. Wan, H. F. Yang, D. Y. Zhao, *Acc. Chem. Res.* **2006**, *39*, 423.
[31] C. D. Liang, K. L. Hong, G. A. Guiochon, J. W. Mays, S. Dai, *Angew. Chem.* **2004**, *116*, 5909; *Angew. Chem. Int. Ed.* **2004**, *43*, 5785.
[32] S. Tanaka, N. Nishiyama, Y. Egashira, K. Ueyama, *Chem. Commun.* **2005**, 2125.

  

[33] Y. Meng, D. Gu, F. Q. Zhang, Y. F. Shi, H. F. Yang, Z. Li, C. Z. Yu, B. Tu, D. Y. Zhao, *Angew. Chem.* **2005**, *117*, 7215; *Angew. Chem. Int. Ed.* **2005**, *44*, 7053.
[34] C. D. Liang, S. Dai, *J. Am. Chem. Soc.* **2006**, *128*, 5316.
[35] F. Q. Zhang, D. Gu, T. Yu, F. Zhang, S. H. Xie, L. J. Zhang, Y. H. Deng, Y. Wan, B. Tu, D. Y. Zhao, *J. Am. Chem. Soc.* **2007**, *129*, 7746.
[36] C. D. Liang, Z. J. Li, S. Dai, *Angew. Chem.* **2008**, *120*, 3754; *Angew. Chem. Int. Ed.* **2008**, *47*, 3696.
[37] D. Gu, H. Bongard, Y. H. Deng, D. Feng, Z. X. Wu, Y. Fang, J. J. Mao, B. Tu, F. Schüth, D. Y. Zhao, *Adv. Mater.* **2010**, *22*, 833.
[38] J. C. Yu, X. L. Hu, Q. Li, L. Z. Zhang, *Chem. Commun.* **2005**, 2704.
[39] S. H. Yu, X. J. Cui, L. L. Li, K. Li, B. Yu, M. Antonietti, H. Colfen, *Adv. Mater.* **2004**, *16*, 1636.
[40] X. M. Sun, Y. D. Li, *Angew. Chem.* **2004**, *116*, 607; *Angew. Chem. Int. Ed.* **2004**, *43*, 597.
[41] Q. Wang, H. Li, L. Q. Chen, X. J. Huang, *Carbon* **2001**, *39*, 2211.
[42] D. H. Long, F. Lu, R. Zhang, W. M. Qiao, L. Zhan, X. Y. Liang, L. C. Ling, *Chem. Commun.* **2008**, 2647.

  